Attractive membrane domains control lateral diffusion

Martin B. Forstner,[1,2,*] Douglas S. Martin,[1,2,†] Florian Rückerl,[2] Josef A. Käs,[2] and Carsten Selle[2]
[1]*Center for Nonlinear Dynamics, University of Texas, R. L. Moore Building, Austin, Texas 78712, USA*
[2]*Institute of Experimental Physics I, University of Leipzig, Linnéstrasse 5, Leipzig D-04103, Germany*
(Received 21 November 2007; revised manuscript received 1 April 2008; published 9 May 2008)

Lipid membranes play a fundamental role in vital cellular functions such as signal transduction. Many of these processes rely on lateral diffusion within the membrane, generally a complex fluid containing ordered microdomains. However, little attention has been paid to the alterations in transport dynamics of a diffusing species caused by long-range interactions with membrane domains. In this paper, we address the effect of such interactions on diffusive transport by studying lateral diffusion in a phase-separated Langmuir phospholipid monolayer via single-particle tracking. We find that attractive dipole-dipole interactions between condensed phase domains and diffusing probe beads lead to transient confinement at the phase boundaries, causing a transition from two- to one-dimensional diffusion. Using Brownian dynamics simulations, the long-term diffusion constant for such a system is found to have a sensitive, Boltzmann-like, dependence on the interaction strength. In addition, this interaction strength is shown to be a strong function of the ratio of domain to particle size. As similar interactions are expected in biological membranes, the modulation of diffusive transport dynamics by varying interaction strength and/or domain size may offer cells selective spatial and temporal control over signaling processes.

DOI: 10.1103/PhysRevE.77.051906 PACS number(s): 87.15.Vv, 05.40.−a, 87.15.K−, 87.16.D−

I. INTRODUCTION

The physical phenomenon of lateral diffusion within membranes plays a key role in many aspects of cellular life as biochemical reaction-diffusion processes underlie typical cellular signaling cascades [1]. Cytochrome-mediated electron transport [2], photoinactivation of alpha-amino-3-hydroxy-5-methyl-4-isoxazolepropionic acid (AMPA) receptors [3], serotonin receptor signaling [4], and gating of cardiac potassium channels [5] are but a few examples that strongly depend on lateral diffusion of participating molecules through cellular membranes. They underscore the importance of diffusive transport within membranes for proper cell function in general, and in inter- and intracellular signaling in particular [6]. However, the lipid membranes of the cell are not simple objects: they are complex, two-dimensional fluids [7] with spatial and temporal structures such as lipid microdomains, which range in size from one to hundreds of nanometers [8,9]. Also, membranes are electrostatically inhomogeneous [10] and their local properties can be altered by changes, e.g., in composition [11]. Since membrane molecule dimensions of a few nanometers are close to the Debye screening length at physiological conditions, interactions between molecules with permanent dipoles or charges [12] and extended membrane structures are feasible [13]. An important aspect of understanding the control and organization of cellular information transfer is understanding the physics of lateral diffusion in such complex environments. This requires consideration of both the finite size of membrane domains and interactions between domains and diffusing molecules. So far, the effect of geometric constraints alone or point traps on diffusion has been studied in detail [14,15]. However, in the context of a more realistic picture of cellular membranes, a new question regarding the basic physics of diffusion within complex, two-dimensional (2D) fluids arises: How is the diffusion of a particle affected by long-range interactions with extended spatial structures?

In this study, which extends previously reported work from our group [16], we focus on attractive dipole-dipole interactions and show that potentials of a few k_BT are sufficient to transiently confine a diffusing particle to domain boundaries. We show that this confinement temporarily reduces the dimensionality of the diffusive processes from two to one dimension. For a systematic study of diffusion processes over the broadest range of time scales, numerical simulations were employed. These reveal a sensitive dependence on the interaction strength: small differences in the potential result in order of magnitude changes in the long-term diffusion coefficient. In addition, the interaction strength can be easily altered by changing the domain size independent of domain composition. In contrast to earlier work [16], we present a simple physical model that agrees qualitatively and quantitatively with experiment and simulation. This model allows us to connect our findings to the underlying biological membranes, as these phenomena provide a mechanism by which cells can exert selective spatial and temporal control over diffusion based processes such as signal propagation.

II. EXPERIMENTAL DESIGN AND RATIONALE

To understand key aspects of diffusion in structured two-dimensional fluids, a simplified model of the cell membrane was used. We take advantage of the fact that lateral diffusion

*Corresponding author. Present address: University of California, Berkeley, Chemistry Department, Lewis Hall 123, Berkeley, California 94720-1460. FAX: (510) 643-6232. mbf@berkeley.edu
†Corresponding author. Present address: Lawrence University, Physics Department, Appleton, Wisconsin 54912. FAX: (920) 832-6962. Douglas.S.Martin@lawrence.edu

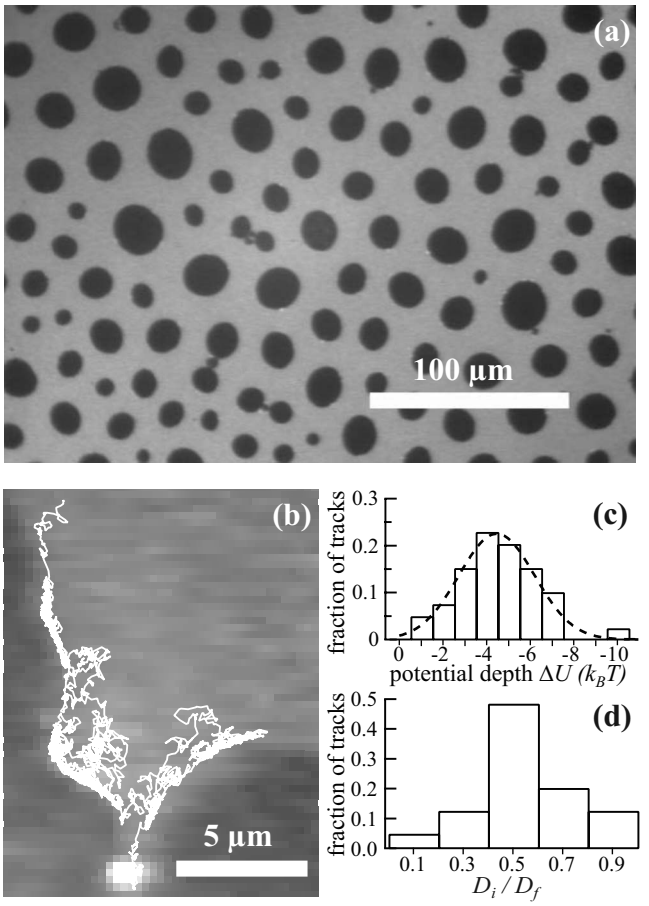

FIG. 1. Effect of attractive domains on diffusion. (a) A representative fluorescence image of a DMPE monolayer exhibiting separation into fluid (light gray) and solid (dark gray) phases. (b) A bead (bright spot) embedded in such a monolayer. 200 s of the bead track (white line) is overlaid, clearly showing the bead attraction to the domain boundaries. (c) Histogram of attractive potential strengths between bead and solid domain ($n=39$ experiments included) is well fitted by a Gaussian (dashed line) with a mean of $-4.5k_BT$. (d) The peak at 0.5 of the ratio of the diffusion coefficient near (D_i) and far (D_f) from the interface marks a transition from 2D to 1D diffusion.

in membranes is, in general, similar to lateral diffusion in monolayers [17]. Instead of a native membrane with thousands of constituents, a monolayer with one type of phospholipid, dimyristoyl phosphatidylethanolamine (DMPE), spread at the air-water interface in a Langmuir film balance serves as the experimental system [18]. Structure is created by adjusting a movable barrier to increase the packing density of the lipids until phase separation into fluid-like, liquid expanded (LE), and solid-like liquid condensed (LC) domains occurs [Fig. 1(a)]. Diffusion within the LE phase is probed with 100-nm-diameter green fluorescent polystyrene beads which were embedded in the monolayer and do not penetrate the LC domains. An attractive potential between the diffusing probes and the LC domains is generated via a dipole-dipole interaction, with a maximum strength of $-6k_BT$ (for details, see the Appendix). By doping the monolayer with red fluorescent lipids that partition strongly into the LE phase, monolayer structure and bead positions were simultaneously recorded at 30 frames per second using video microscopy. Finally, bead positions are determined in each frame and assembled into tracks as described in Sec. V B.

III. RESULTS AND DISCUSSION

A. Confinement of probe beads at domain boundaries

The effect of an attractive interaction between domains and probes is immediately visible in the overlay of a bead track and the corresponding monolayer structure shown in Fig. 1(b): The probe's diffusive motion is partially confined at the LC domain boundary. The magnitude of the underlying interaction can be extracted by calculating the average potential U in proximity to the interface, assuming the bead reaches equilibrium, i.e., the bead positions follow a Boltzmann distribution $\rho(r) \propto \exp[-U(r)/k_BT]$, where r is the bead distance from the interface and ρ is the density of bead positions. Our experimental resolution distorts the precise shape of the potential, but the potential depth ΔU can be computed from the density of bead positions near and far from the boundary using

$$\Delta U = U(r=0) - U(r>2\sigma) = \ln\left(\frac{\rho(r>2\sigma)}{\rho(r=0)}\right)k_BT, \quad (1)$$

where σ is the position accuracy of our experiment (~ 0.5 μm). Under our experimental conditions, the potential $U(r)$ for $r>2\sigma$ is far enough from domains to be approximately constant and zero. A histogram of potential depths is shown in Fig. 1(c); the average ΔU of $-(4.5\pm1)k_BT$ agrees well with the theoretical value of $-6k_BT$.

B. Boundary confinement reduces the dimensionality of the diffusion process

The local effect of the bead-domain interaction on bead diffusion was examined by calculating two diffusion coefficients from the mean square displacement (MSD) of the experimental tracks assuming 2D diffusion [19]: D_i for the portions of the track near the interface ($r<2\sigma$) and D_f for the portions far from the boundary ($r>2\sigma$). Interestingly, the average of the ratio D_i/D_f is 0.5 [Fig. 1(d)]. This can be understood by comparing free one- and two-dimensional diffusion characterized by MSDs of $2Dt$ and $4Dt$, respectively. The MSD ratio (equivalent to D_i/D_f) of 0.5 indicates that the attractive domain-probe interaction reduces the dimensionality of the diffusive process from 2D far from the domains to one dimensional at the boundary.

C. Investigations of diffusion in the long-time limit by simulations

Our experiments clearly demonstrate that interaction energies of a few k_BT are sufficient to locally alter diffusive behavior. In living cells, the lifetime of membrane proteins is many hours [20] so the question arises of how diffusion in the long-time limit is affected by the presence of attractive membrane domains. Our experimental system is limited by collective monolayer drift to observations of minutes [18];

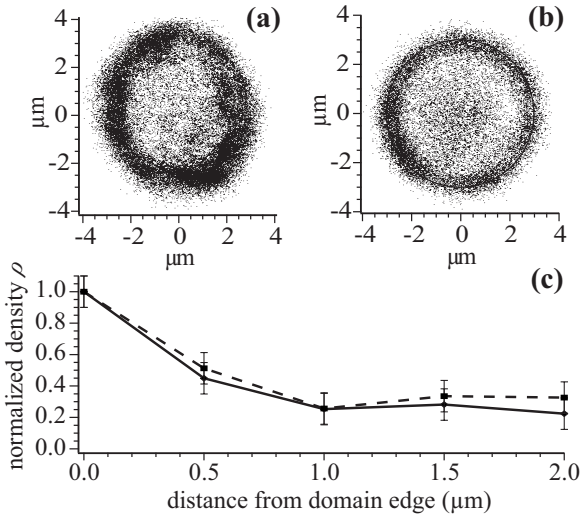

FIG. 2. Comparison of experimental and simulated particle diffusion. (a) Experimental positions of 100 nm bead diffusing in fluid region of 3 μm radius, surrounded by solid phase lipids (1000 s track). (b) Simulation of bead under experimental conditions including noise (potential depth $-5k_BT$). The black ring indicates the edge of the fluid phase domain (3 μm radius). Points outside the boundary are due to the noise profile which matches the experimental conditions. (c) Comparison of density of experiment (solid line) and simulation (dashed line) as a function of distance from the edge of the domain. The relative drop in density ρ is smaller than predicted by a $-5k_BT$ potential due to smearing of particle positions by noise.

hence 2D Brownian dynamics simulations were used to access longer times. In short, the particle undergoes a discrete time random walk, with the displacement at each time given by a random (Brownian) component and a directed component due to the dipole-dipole interaction. In order to match the experimental conditions, the free diffusion coefficient of the bead and the friction coefficient were set to $D_f=1$ μm^2/s and $\xi=k_BT/D_f$, respectively.

To validate our simulation, we compare numerical and experimental results in Fig. 2. The experimental track of a bead diffusing in a circular LE domain (3 μm radius) surrounded by LC phase is depicted in Fig. 2(a), while Fig. 2(b) shows a simulated track in the same geometric configuration. In both cases the confinement at the interface is clearly visible. Likewise, experiment and simulation show the same bead density profile as a function of the distance from the interface [Fig. 2(c)]; this agreement indicates that the simulations accurately reproduce the experimental system. In the following we describe simulation results, followed by a discussion of their physical origins.

D. Passive versus attractive domains

Employing this simulation scheme, we first compare diffusion in the limits of no domains, domains with no interaction potential, and domains with a large attractive potential ($-10k_BT$). The domain array of the latter two cases consists of circular domains of 2 μm radius spaced 10 μm apart. Random walks are simulated for a total of 90 000 s allowing us to examine short- and long-time behavior.

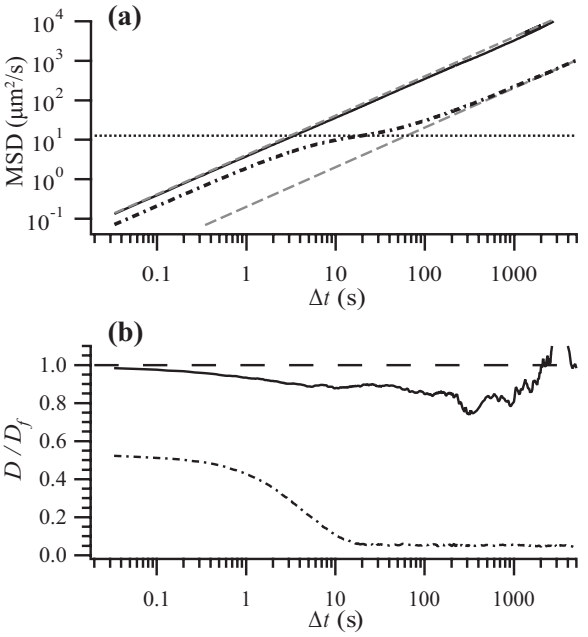

FIG. 3. MSD and diffusion coefficient from a simulated particle diffusing among solid domains. (a) The MSD of the particle motion among domains with (dash-dotted line) and without (solid line) attractive interactions. Without interactions, the MSD grows linearly (short-dashed gray line, slope=1), and thus remains normal at all times. With interactions, however, normal diffusion at short and long times (long-dashed gray line, slope=1) brackets a range of transient nonlinear growth of the MSD with time. Dotted line: Area corresponding to one domain. (b) Corresponding normalized diffusion coefficients. Dashed line: no domains. A particle diffusing among domains without interactions (solid line) is influenced only slightly while attractive interactions have a significant impact on diffusion (dash-dotted line). The variability at long times is due to limited statistics.

The time-dependent MSDs for all scenarios are calculated from the tracks of the diffusing particles as described [19] and presented in Fig. 3(a). Compared to the strict linear growth of the MSD for free diffusion, the MSD in the case of passive obstruction shows only a slight deviation at long times, as expected [15]. Qualitatively different, however, is the behavior of the MSD in the presence of an attractive interaction between the domains and the random walker. Following an initial linear growth phase, the MSD plateaus at approximately the domain size, indicating transient confinement. The MSD resumes a linear increase at longer times, indicating a return to normal diffusion [21] with a smaller diffusion coefficient.

This strong modulation of diffusive behavior by attractive domains is apparent in the normalized diffusion coefficients $D(\Delta t)$ depicted in Fig. 3(b). Diffusion coefficients are normalized with respect to D_f, the free diffusion coefficient, following $D(\Delta t)/D_f=[\mathrm{MSD}(\Delta t)/4\Delta t]/D_f$. In the case of passive domains, $D(\Delta t)$ only differs from D_f by an amount comparable to the area fraction of the domains [15]. In contrast, with attractive domains the initial diffusion coefficient ratio of 0.5 declines rapidly by an order of magnitude, demonstrating the large impact of attractive obstacles on diffusion.

Previous studies on diffusion properties in phase-separated membranes report a reduction in the diffusion coefficients that is directly related to an increase of the area fraction of the impermeable gel-phase membrane [22,23]. In good agreement with theoretical predictions, they show that diffusion coefficients go to zero as the gel-phase area fraction approaches the percolation threshold. In contrast, the system modeled by our simulations is far from the percolation threshold (the area fraction of domains is 0.125). The solid line in Fig. 3(b) representing diffusion through the purely obstructed system (no interactions), exhibits the predicted decline of a few percent. Thus, the dramatic slowing of diffusive propagation that we find in the presence of interactions is not caused by geometric effects, but can indeed be traced back to increased residence times of the diffusing probe at the domain boundaries as elaborated in more detail below.

As the dashed line in Fig. 3(a) indicates, the long-term diffusive behavior in our simulated system is normal (i.e., the MSD grows linearly with time). The bend in the MSD vs Δt plot for simulated interaction (dash-dotted line) does not indicate anomalous diffusion [24]. It occurs at an intermediate time scale that connects two regimes of normal diffusion with dissimilar diffusion coefficients. Such time scales characterized by temporary diffusion coefficients in membrane systems have been previously reported [23]. However, experimental evidence in such systems for true anomalous subdiffusion, which is signified by a sublinear growth of the MSD in the long-time limit, has not been reported. In the context of biological cells, this distinction is not necessarily fruitful as only particular time scales are relevant. Both intermediate regimes as described above and true anomalous subdiffusion will lead to a similar result: slower spread of molecules and, therefore, stronger localization of the diffusive species.

E. Diffusion coefficient as function of potential depth

To investigate the effect of a transition from passive to attractive domains on the long-time diffusion coefficient D_∞, simulations were performed with a range of potential strengths. The resulting ratios D_∞/D_f for simulations with the same geometrical arrangement as above are shown in Fig. 4. The coefficient ratio is well fitted by a curve of the form

$$\frac{D_\infty(\Delta U)}{D_f} = \frac{1}{1+\exp[-A(\Delta U - U_h)/k_BT]}, \qquad (2)$$

where U_h, the inflection point of the curve, and A are fitting parameters (here $A=0.79\pm0.14\approx1$). The potential strength of $U_h=-(6.7\pm0.7)k_BT$ marks the sharp transition from almost unaltered free diffusion to a diffusive process with a drastically reduced diffusion coefficient. In other words, two diffusing species with only a small difference in their interactions with domains will propagate significantly differently in the same environment.

F. Effect of domain size

In the particular case of dipole-dipole interactions, the potential $U(\mathbf{r})$ is not completely independent of domain and particle dimension. Small domains create an electric dipole field similar to a point dipole, where the electric field $E(\mathbf{r})$, and hence $U(\mathbf{r})$, scales with the distance r from the domain as $1/r^3$. In contrast, large domains are well approximated by semi-infinite dipole sheets with an electric field and potential that scale as $1/r$. For intermediate domain sizes, the distance dependence of the potential smoothly varies between these two limiting cases [16]. Because the point of closest approach is the radius of the diffusing particle, the potential depth at the interface depends on the scaling of the potential. Therefore, particles diffusing near smaller domains are subject to a reduced potential depth, as shown in Fig. 5. Domain size alone, independent of domain composition, therefore allows the long-term diffusion coefficient to be controlled according to Eq. (2) and Fig. 4.

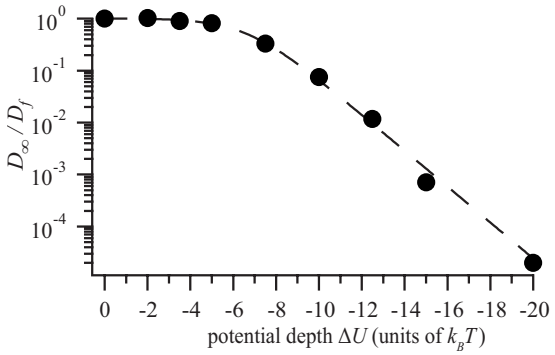

FIG. 4. Normalized long-time diffusion coefficient as a function of potential depth. A sharp transition from free diffusion to slowed diffusion is apparent at a potential depth of about $-6k_BT$ (note the logarithmic scale on the y axis). The dashed line is the fit to Eq. (2).

G. Physical origins of the modulation of the diffusion behavior by attractive domains

The striking features in diffusive behavior that emerge in the presence of attractive domains—both the drop in the diffusion coefficient at intermediate times (Fig. 3) and the sensitive dependence of the diffusion coefficient on the potential strength at long times (Fig. 4)—can be explained by considering the underlying physical mechanisms:

At short times, motion is dominated by 1D diffusion along domain boundaries resulting in a $D(\Delta t)/D_f$ ratio of 0.5 [as in Fig. 1(c)]. Owing to the entrapment at the boundary, the particle appears confined at intermediate times, so $D(\Delta t)/D_f$ drops as the particle explores a significant portion of the domain boundary ($\pi d^2/D_f \sim 10$ s, where d is the domain radius). At long times the domains can be approximated as point traps. Hence, D_∞ is determined by the fraction of time the particle diffuses freely (D_f) between the domains: $D_\infty = D_f[\tau_f/(\tau_f+\tau_s)]$, where τ_f is the average time a particle spends freely diffusing and τ_s is the average residence time at domain boundaries, given by $\tau_s = C\exp(-\Delta U/k_BT)$. Together one recovers the functional form for the ratio D_∞/D_f given in Eq. (2), with $C/\tau_f = \exp(U_h/k_BT)$ in the approximation $A=1$. Thus, the sensitivity of D_∞ to the potential is a direct result of the Boltzmann distribution of bead residence times at domain boundaries. This modulation of the diffusion

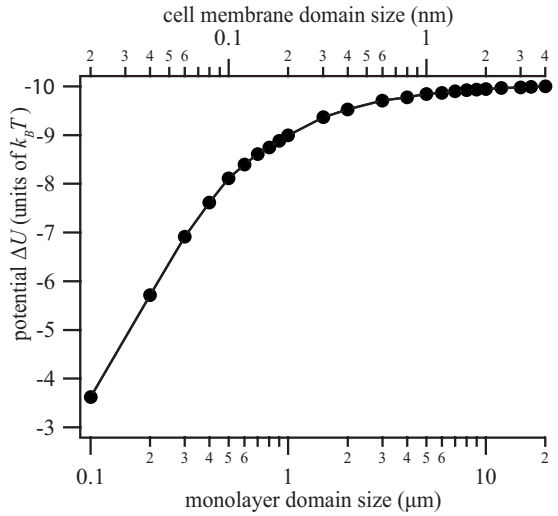

FIG. 5. Calculated potential depth as a function of domain size, for both a 100 nm bead in the monolayer system (bottom axis) and a 2 nm protein in a cell membrane (top axis). The sharp drop at small domain sizes indicates a potential mechanism to modulate diffusive dynamics. The line represents a linear interpolation between data points.

behavior is therefore not specific to the dipole-dipole interaction but will occur in the presence of any suitable interaction between domains and diffusing particle.

H. Scale invariance and consideration of cellular dimensions

As shown above, the changes in diffusion coefficient depend on the potential strength alone. In addition, the geometric effects of domain size depend only on the ratio of particle to domain size. This allows us to rescale the interaction we observe down from experimental to cellular scales, where diffusive behavior of membrane proteins or protein clusters will be affected (Fig. 5). Because the observed effects do not depend on the particular nature of the interactions, similar phenomena could arise from other attractive forces, e.g., stemming from hydrophobic mismatch [25]. However, the results from monolayer studies described in this article are particularly relevant for scenarios in which membrane domains are asymmetric and/or occur only on one leaflet of the lipid bilayer. Because of the strong compositional asymmetry between the two leaflets of plasma membranes, it is not surprising that membrane heterogeneities are often found to also be asymmetric with respect to cytosolic and extracellular membrane leaflet [26].

For example, lipid rafts are thought to be cholesterol-enriched domains which exist on scales of one to hundreds of nanometers [9]. These domains in biological membranes are often found to be asymmetric across the bilayers [26,27]. Thus, it seems plausible that such domains display net dipole moments similar to those in monolayers where excess dipole densities of about 0.85 D/nm^2 [28] have been measured for cholesterol-enriched domains. Raft-associated membrane proteins such as *E*-cadherin and neutral cell adhesion molecule (NCAM) are predicted to have large dipole moments (~1500 D [29]), considering a typical protein diameter of ~2 nm and a domain size of 100 nm, we estimate the potential depth for this protein-domain interaction to be $\sim 10 k_B T$, directly in the transition region of Fig. 4. As with larger particles and domains, the potential depends on the size of the domains, as shown in Fig. 5 (top axis). A small change in domain size leads to a large change in potential strength, and consequently diffusive behavior.

IV. CONCLUSION AND BIOLOGICAL PERSPECTIVE

In this study we show that attractive domains can strongly affect diffusion processes. Interaction potentials of a few $k_B T$ give rise to several interesting phenomena: intermittent confinement of the diffusing particle at the domain boundaries, reduction in dimensionality of the resulting diffusing process, and a potential-sensitive modulation of long-range diffusion. Since these features are independent of the details of the interaction, they should be of general nature and appear in all 2D fluids of similar makeup.

In the cellular context, where physical properties can influence and even determine biological function, the mechanisms described in this study may lead to intriguing consequences. Because the amino acid sequence and structure of a protein determine its electrostatic properties and thus its particular interaction strength with membrane domains, the effects of domain-protein attraction will be specific to each molecular species. This provides a selective mechanism to allow for free diffusion of molecules with low or no attraction to domains, while enriching proteins with strong interactions at domain boundaries. Together with the reduction of such molecules' motion to one dimension, biochemical reaction rates can be significantly enhanced [30]. In addition, by decreasing their overall diffusive speed, molecules attracted by domains remain localized while molecules without domain interaction experience only passive obstruction and propagate much faster. Thus, by invoking domain-protein interactions, different proteins embedded in the same membrane environment can exhibit very dissimilar dynamic and kinetic properties. In turn, these molecule-specific lateral mobilities and kinetic rates will change as the membrane environment is modified by the cell, e.g., by changes in domain sizes or alterations to membrane composition. Therefore, the physical phenomena reported in this work provide the foundation of a potential mechanism for living cells to specifically control membrane associated reaction-diffusion processes and ultimately biological function.

V. MATERIALS AND METHODS

A. Vesicle suspension and bead conjugation

DMPE (Avanti Lipids, Alabaster AL) was mixed with 0.5 mol % Texas-Red-labeled 1,2-dipalmitoyl-*sn*-glycero-3-phosphoethanolamine (DPPE) (Invitrogen Corporation, Carlsbad, CA), in a 2:1 chloroform to methanol solution. The mixture was spread on a Teflon plate (3 cm diameter) placed in a 50 ml glass beaker and dried under a vacuum for 6 h. The dried lipids were hydrated with 5 ml phosphate-buffered saline (100 m*M*, potassium-free, *p*H 7.5) and heated at 55 °C for at least 8 h to allow vesicle formation. To create

small unilamellar vesicles (SUVs), the lipid suspension was sonicated using a sonic dismembrator (Fisher Scientific, Pittsburgh, PA), which reduces the average diameter of the vesicles from several micrometers to a few hundred nanometers and facilitates a rapid (2–4 h) formation of the monolayer.

Carboxylated yellow-green fluorescent polystyrene spheres (100 nm diameter, from Invitrogen Corporation, Carlsbad, CA) were diluted with the PBS buffer to 0.001% solids and sonicated for 1 min; immediately afterward, the solution was spun at 100 000*g* for 5 min to sediment remaining aggregates; only the supernatant was subsequently used. The SUV suspension and the bead solution were mixed in a 1:1 volume ratio, briefly vortexed, and conjugated at room temperature for 2 h. The vesicle-bead solution was diluted in PBS buffer, vortexed, and centrifuged at 100 000*g* for 5 min to remove free beads, which remain in suspension. The pellet, containing the bead-labeled vesicles, was resuspended in 2 ml of PBS. Lipid monolayers were formed from the bead-vesicle solution on a custom-built Langmuir film balance described in detail in [18]. Monolayers were compressed into the LE-LC coexistence region (typical surface tension 15 mN/m after compression at less than 1 mm/min); experiments were performed at room temperature (22 ± 2 °C).

B. Video microscopy, image analysis, single-particle tracking, and density calculation

The monolayer was observed using an upright fluorescence microscope (Olympus BX-FLA, 50×0.8 numerical aperture, fluorescence and dark field objective, Center Valley, PA) equipped with afluorescein isothiocyanate (FITC)–Texas Red dual fluorescence filter set (51006, Chroma, Brattleboro, VT). Images were acquired with a silicon intensified tube (SIT) camera (Dage-MTI VE-1000 SIT, Michigan City, IN; field of view, approximately 300×200 μm^2) at 30 frames per second, digitized (National Instruments PCI 1407, Austin, TX), and stored on a hard drive array in real time. About 10–50 particles were tracked at once with an accuracy of 500 nm using the method described in [31]. The position data were corrected for spatial distortions introduced by the radially increasing pixel size and the rectangular pixel shape of the SIT camera before further analysis.

Since the interaction potential rapidly assumes a constant value with increasing distance from the domain boundary, regions far away from domain edges do not contain information about the spatial dependence of $U(r)$. It is therefore sufficient to calculate the number density $\rho(r)$ as a function of the distance r via $\rho(r)=n(r)/A(r)$ within the proximity of a domain. To count the number of particles, $n(r)$, and the corresponding area $A(r)$ at a distance r from a domain edge, the space surrounding a domain was subdivided into sections. To that end, strips of 0.5 μm ($\approx\sigma$, the positional precision) depth, running parallel to the domain edge, were further divided into sections of 0.5 μm width. For each particle trajectory the total number of particle positions within sections with a particular r was counted. Similarly, the number of sections at the same distance r that were traversed by the trajectory gave an approximate measure for the area $A(r)$ which accounts for the geometric configuration.

C. Numerical simulations

At each time step δt, the 2D displacement of the bead $\Delta\mathbf{r}$ is calculated as the sum of a Brownian displacement $\Delta\mathbf{r}_B$ and an additional displacement $\Delta\mathbf{r}_F$ due to the dipole-dipole interaction. $\Delta\mathbf{r}_B$ is obtained by choosing a random angle from $[0, 2\pi]$ and a step size r from $P(r)=(1/4\pi D_f \delta t)\exp(-r^2/4D_f\delta t)$. The displacement $\Delta\mathbf{r}_F$ due to a force $\mathbf{F}(\mathbf{r})$ is given by $\Delta\mathbf{r}_F=\delta t\mathbf{F}(\mathbf{r})/\xi$, ξ the friction coefficient, in the limit $\mathbf{F}(\mathbf{r})$ is constant over $\Delta\mathbf{r}_F$. Hence, first the dipole-dipole potential $\mathbf{U}(\mathbf{r})$ is evaluated (see the Appendix) with the force acting on the bead calculated via $\mathbf{F}(\mathbf{r})=-\nabla U(\mathbf{r})$. We adaptively adjust δt such that $\mathbf{F}(\mathbf{r})$ is approximately constant over $\Delta\mathbf{r}=\Delta\mathbf{r}_B+\Delta\mathbf{r}_F$ $\{P(\Delta r)<10^{-6}$ for $[\mathbf{F}(\mathbf{r}+\Delta\mathbf{r})-\mathbf{F}(\mathbf{r})]/\mathbf{F}(\mathbf{r})>0.02\}$ resulting in time steps from 0.033 s (far from domains) down to 10^{-6} s (near domains). If the particle track intersects the solid domain boundary during $\Delta\mathbf{r}$, it is reflected back into the fluid phase. For direct comparison with experiments (Fig. 2), the simulated walks are resampled at 30 Hz and convolved with a noise profile which was determined from images from the monolayer experiments.

ACKNOWLEDGMENTS

We are indebted to Dr. H. Swinney for his support and advice and to Dr. M. Saxton for fruitful discussions. This work was supported by the DFG, Grant No. KA-1116/4-1 to C.S. and J.A.K.

APPENDIX: DIPOLE-DIPOLE POTENTIAL BETWEEN PROBE BEAD AND DOMAINS

The potential energy $U(\mathbf{r})$ of a bead embedded in the monolayer at position $\mathbf{r}$ is given by $U(\mathbf{r})=\boldsymbol{\mu}_b\cdot\mathbf{E}(\mathbf{r})$, with $\boldsymbol{\mu}_b$ the dipole moment of the bead and $\mathbf{E}(\mathbf{r})$ the electric field due to the solid phase domains. The dipole moment μ_b for a half-submerged carboxyl coated polystyrene bead is perpendicular to the monolayer, and is approximately [32] 9×10^5 D, using $\mu_b \approx \pi a^2 \bar{q}_b \lambda_d$, with a the bead radius of 50 nm, $\bar{q}_b$ the surface charge density of the bead of 3.38 e/nm^2, and λ_d the Debye screening length in the PBS subphase [pH 7.5, ionic strength of 0.189 mol/l, $\lambda_d \approx (0.3\ \mathrm{nm})/\sqrt{0.189} \approx 0.7$ nm]. The electric field perpendicular to the monolayer is given by

$$E(\mathbf{r}) = \int p/4\pi\varepsilon|\mathbf{r}-\mathbf{r}_0|^3 dr_0, \tag{A1}$$

with $p=50$ mD/nm^2 the dipole density difference between the solid phase and the fluid phase [33], $\mathbf{r}_0$ the solid domain radius, and ε the dielectric constant of the monolayer, approximately $7\varepsilon_0$. This value is in excellent agreement with the recently published value of $\sim 10\varepsilon_0$, stemming from numerical simulations [34]. $E(\mathbf{r})$ was integrated numerically for arbitrary domain sizes and the resulting $U(\mathbf{r})$ for the experimental configuration was found to have a depth of $-6k_BT$ at one bead radius (point of closest approach), and a width $[U(\mathbf{r})<1k_BT]$ of $\sim$200 nm (essentially independent of domain shape for domains much larger than the bead).

[1] U. S. Bhalla and R. Iyengar, Science **283**, 381 (1999); B. N. Kholodenko, Nat. Rev. Mol. Cell Biol. **7**, 165 (2006).
[2] S. Kim, T. Yamamoto, Y. Todokoro, Y. Takayama, T. Fujiwara, J. S. Park, and H. Akutsu, Biophys. J. **90**, 506 (2006).
[3] H. Adesnik, R. A. Nicoll, and P. M. England, Neuron **48**, 977 (2005).
[4] T. J. Pucadyil and A. Chattopadhyay, Glycoconjugate J. **24**, 25 (2007).
[5] H. Cho, Y. A. Kim, J. Y. Yoon, D. Lee, J. H. Kim, S. H. Lee, and W. K. Ho, Proc. Natl. Acad. Sci. U.S.A. **102**, 15241 (2005).
[6] P. D. Calvert, V. I. Govardovskii, N. Krasnoperova, R. E. Anderson, J. Lem, and C. L. Makino, Nature (London) **411**, 90 (2001); D. Choquet and A. Triller, Nat. Rev. Neurosci. **4**, 251 (2003).
[7] D. M. Engelman, Nature (London) **438**, 578 (2005); A. Kusumi, C. Nakada, K. Ritchie, K. Murase, K. Suzuki, H. Murakoshi, R. S. Kasai, J. Kondo, and T. Fujiwara, Annu. Rev. Biophys. Biomol. Struct. **34**, 351 (2005); D. Marguet, P. F. Lenne, H. Rigneault, and H. T. He, EMBO J. **25**, 3446 (2006).
[8] D. A. Brown and E. London, J. Biol. Chem. **275**, 17221 (2000).
[9] K. Jacobson, O. G. Mouritsen, and R. G. W. Anderson, Nat. Cell Biol. **9**, 7 (2007).
[10] M. Olivotto, A. Arcangeli, M. Carla, and E. Wanke, Bioessays **18**, 495 (1996); T. Yeung, M. Terebiznik, L. M. Yu, J. Silvius, W. M. Abidi, M. Philips, T. Levine, A. Kapus, and S. Grinstein, Science **313**, 347 (2006).
[11] T. Starke-Peterkovic, N. Turner, M. F. Vitha, M. P. Waller, D. E. Hibbs, and R. J. Clarke, Biophys. J. **90**, 4060 (2006).
[12] T. Simonson, Rep. Prog. Phys. **66**, 737 (2003).
[13] S. McLaughlin and D. Murray, Nature (London) **438**, 605 (2005).
[14] S. Havlin and D. Ben-Avraham, Adv. Phys. **51**, 187 (2002); T. V. Ratto and M. L. Longo, Biophys. J. **83**, 3380 (2002); M. J. Saxton and K. Jacobson, Annu. Rev. Biophys. Biomol. Struct. **26**, 373 (1997); K. Tamada, S. H. Kim, and H. Yu, Langmuir **9**, 1545 (1993); M. A. Deverall, E. Gindl, E. K. Sinner, H. Besir, J. Ruehe, M. J. Saxton, and C. A. Naumann, Biophys. J. **88**, 1875 (2004).
[15] M. J. Saxton, Biophys. J. **39**, 165 (1982).
[16] C. Selle, F. Ruckerl, D. S. Martin, M. B. Forstner, and J. A. Kas, Phys. Chem. Chem. Phys. **6**, 5535 (2004).
[17] M. B. Forstner, J. Kas, and D. Martin, Langmuir **17**, 567 (2001); P. C. Ke and C. A. Naumann, *ibid.* **17**, 3727 (2001).
[18] M. B. Forstner, D. S. Martin, A. M. Navar, and J. A. Kas, Langmuir **19**, 4876 (2003).
[19] H. Qian, M. P. Sheetz, and E. L. Elson, Biophys. J. **60**, 910 (1991).
[20] D. W. Laird, Biochim. Biophys. Acta **1711**, 172 (2005) ; T. U. Park, L. Lucka, W. Reutter, and R. Horstkorte, Biochim. Biophys. Acta **234**, 686 (1997).
[21] M. J. Saxton, Biophys. J. **70**, 1250 (1996).
[22] P. F. F. Almeida, W. L. C. Vaz, and T. E. Thompson, Biochemistry **31**, 7198 (1992); A. Arnold, M. Paris, and M. Auger, Biophys. J. **87**, 2456 (2004).
[23] T. V. Ratto and M. L. Longo, Langmuir **19**, 1788 (2003).
[24] J. P. Bouchaud and A. Georges, Phys. Rep. **195**, 127 (1990).
[25] R. G. W. Anderson and K. Jacobson, Science **296**, 1821 (2002).
[26] P. F. Devaux and R. Morris, Traffic **5**, 241 (2004).
[27] V. Kiessling, J. M. Crane, and L. K. Tamm, Biophys. J. **91**, 3313 (2006).
[28] D. J. Benvegnu and H. M. McConnell, J. Phys. Chem. **97**, 6686 (1993).
[29] From http://bip.weizmann.ac.il/dipol/index.html for Protein Database entries 1QZ1 and 1FF5; based on C. E. Felder, S. A. Botti, S. Lifson, I. Silman and J. L. Sussman, J. Mol. Graphics Modell. **15**, 318 (1997).
[30] A. V. Barzykin, K. Seki, and M. Tachiya, Adv. Colloid Interface Sci. **89-90**, 47 (2001).
[31] J. C. Crocker and D. G. Grier, J. Colloid Interface Sci. **179**, 298 (1996).
[32] P. Nassoy, W. R. Birch, D. Andelman, and F. Rondelez, Phys. Rev. Lett. **76**, 455 (1996).
[33] A. Miller, C. A. Helm, and H. Mohwald, J. Phys. **48**, 693 (1987).
[34] J. Wohlert and O. Edholm, Biophys. J. **87**, 2433 (2004).